Critical Behavior of the Ferromagnetic Perovskite $BaRuO_3$

J.-S. Zhou,[1,2,*] K. Matsubayashi,[1] Y. Uwatoko,[1] C.-Q. Jin,[3] J.-G. Cheng,[2] J. B. Goodenough,[2] Q. Q. Liu,[3] T. Katsura,[4] A. Shatskiy,[4] and E. Ito[4]

[1]*Institute for Solid State Physics, University of Tokyo, Kashiwa, Japan*
[2]*Texas Materials Institute, University of Texas at Austin, Austin, Texas 78712, USA*
[3]*Institute of Physics, Chinese Academy of Science, Beijing 100080, China*
[4]*Institute for Study of the Earth's Interior, Okayama University, Tottori-ken, Japan*

(Received 26 March 2008; published 15 August 2008)

A thorough study has been made of the physical properties under high pressure of the perovskite $BaRuO_3$ synthesized under pressure; it includes the critical behavior in the vicinity of T_c to 1 GPa and the temperature dependences of resistivity and ac magnetic susceptibility up to 8 GPa. The ferromagnetism in $BaRuO_3$ is suppressed at 8 GPa. Critical fluctuations in the vicinity of T_c have been found in $BaRuO_3$ and they are enhanced under pressure. These observations are in sharp contrast to $SrRuO_3$ where mean-field behavior is found at T_c.

DOI: 10.1103/PhysRevLett.101.077206 PACS numbers: 75.30.Et, 75.10.Lp, 75.40.−s

In a very weak itinerant-electron ferromagnetic (VWIEF) system where the exchange energy separates energies of α spin and β spin slightly, the single-particle excitations can be expanded versus temperature over the temperature range $T/T_F \ll 1$, where T_F is the Fermi temperature. This is the basis for Wohlfarth [1] to derive the relationship

$$M(H, T)^2 = M(0, 0)^2[1 - (T/T_c)^2 + 2\chi_0 H/M(H, T)],$$

which gives parallel lines of the isothermal M^2 versus H/M within $T = T_c \pm \delta$, i.e., the Arrott plot. The VWIEF $ZrZn_2$ is a prototype in this mean-field universality class [2]. However, most metallic ferromagnets covering a broad range of systems such as Ni [3], CrO_2 [4], Sr_2FeMoO_6 [5], and $La_{1-x}A_xMnO_3$ (A = Ca, Sr, Ba) [6–8] show significant critical fluctuations as T_c is approached from T_c^- and T_c^+. In comparison with $ZrZn_2$, the observation of a mean-field behavior near the ferromagnetic transition temperature in the metallic perovskite $SrRuO_3$ [9] is highly unusual since the saturation magnetization at the lowest temperature, although it remains below the spin-only value, is clearly beyond the criterion of "very weak magnetization." Therefore, the mean-field universality class and the ferromagnetism itself found in $SrRuO_3$ may not be rationalized through the procedure that Wohlfarth has used to treat the VWIEF system. The effects of chemical substitution, stress, and hydrostatic pressure may provide some important clue for understanding the peculiar critical behavior of $SrRuO_3$. By studying a thin-film sample of $SrRuO_3$, Klein *et al.* [10] have shown that the epitaxial stress not only lowers T_c by about 10 K but also introduces a totally different universality class of critical fluctuations. Ca doping in the perovskites $Sr_{1-x}Ca_xRuO_3$, however, creates more problems than it helps to solve. Ca substitution suppresses the ferromagnetic state [11]. The complicated isothermal magnetization, perhaps due to variance effects of different electronegativity and ionic size between Ca^{2+} and Sr^{2+}, make an analysis of the critical behavior in perovskites $Sr_{1-x}Ca_xRuO_3$ difficult, if not impossible. As for the end member $CaRuO_3$, it no longer shows any magnetic ordering. The success of synthesizing under high pressure ferromagnetic, cubic $BaRuO_3$ with $T_c = 60$ K brings a new opportunity to reveal the effects of crystal structure and of electronegativity of the A-site ion on the critical behavior. Moreover, we have carried out isothermal $M(H)$ measurements under high pressure in order to find the evolution as a function of pressure of the critical behavior of the perovskite $BaRuO_3$.

Details of high-pressure synthesis and characterizations of the perovskite $BaRuO_3$ can be found in a previous publication [12]. The measurements of isothermal magnetization were carried out in a SQUID magnetometer (Quantum Design). The correction for demagnetization was found to have a negligible influence in determining the final critical exponents. We have dropped this correction in analyzing the isothermal $M(H)$ under pressure since detecting the low-field response from the sample is impossible due to the contribution from the pressure cell. The isothermal $M(H)$ under pressure were measured with a miniature Cu-Be cell fitting the SQUID magnetometer. A piece of Pb as the pressure manometer, the sample, and a mixture of 3M Florinert FC77 + FC70 as the pressure medium were sealed in a Teflon capsule. Measurements of the dc resistivity and the ac magnetic susceptibility under pressure to 8 GPa were carried out with a cubic anvil apparatus [13]; the sample assembly is similar to that used in the Cu-Be cell. The pressure inside the high-pressure chamber was determined by a calibrated curve of pressure versus loading.

As seen in Fig. 1(a), the plot of M^2 versus H/M of the perovskite $BaRuO_3$ at ambient pressure does not give parallel linear lines as expected by mean-field behavior. Instead, a modified Arrott plot of the Heisenberg model gives nearly linear parallel lines for temperatures near T_c at

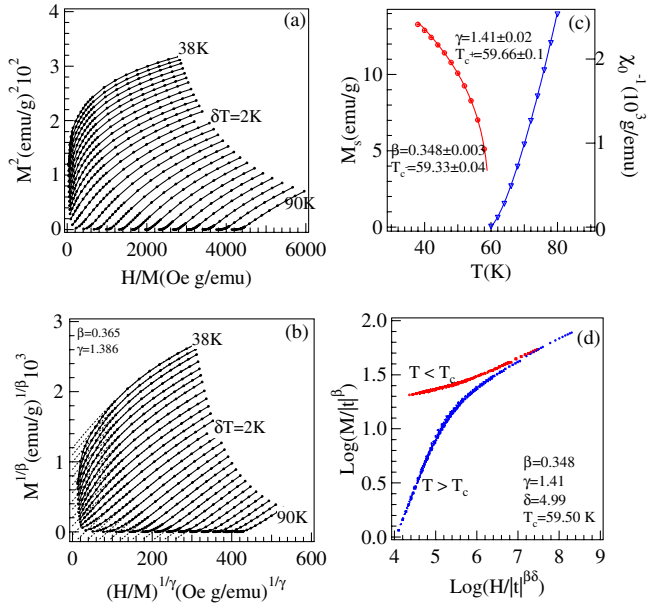

FIG. 1 (color online). (a) The Arrott plot of $M(H)$ of $BaRuO_3$; (b) the modified Arrott plot $M(H)$ with critical parameters of a Heisenberg model; the dashed lines are the curve fitting with polynomial at high magnetic field; (c) temperature dependences of M_s and χ_0^{-1} with power-law fittings; (d) a scaling plot of the $M(H)$ obtained at 38 K $\leq$ T $\leq$ 90 K with the γ and β obtained from the power-law fitting in (c).

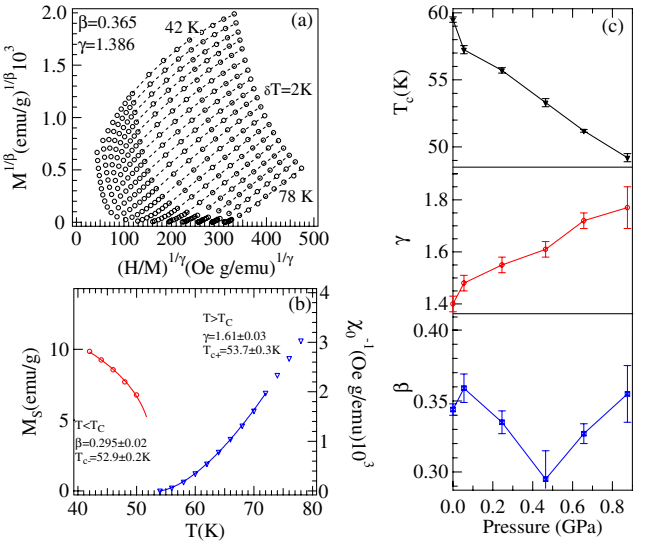

FIG. 2 (color online). (a) The modified Arrott plot of $M(H)$ of $BaRuO_3$ under $P = 0.47$ GPa; (b) temperature dependences of M_s and χ_0^{-1} from the curve fitting in (a); (c) pressure dependences of the critical transition temperature T_c and critical parameters γ and β obtained from the power-law fitting in (b) under different pressures.

which the plot $M^{1/\beta}$ versus $(H/M)^{1/\gamma}$ goes through the origin as shown in Fig. 1(b). The fitting $M^{1/\beta}$ versus $(H/M)^{1/\gamma}$ with a polynomial at high fields gives M_s or χ_0 for each temperature below and above T_c, which is plotted in Fig. 1(c). T_{c+} and T_{c-} obtained from a power-law fitting of M_s vs T and χ_0^{-1} vs T are nearly identical. The scaling plot of Fig. 1(d) obtained by using the fitting parameters from Fig. 1(c) verifies the critical behavior over, at least, the temperature range measured. This feature together with nearly linear lines in the modified Arrott plot indicate that the critical behavior analysis is reliable. Three critical components $\beta = 0.348$ and $\gamma = 1.41$ from Fig. 1 (c) and $\alpha \approx 0.11$ from $d\rho(T)/dT$ [12] fulfill a scaling law $\gamma + 2\beta + \alpha = 2$, which applies generally to fluctuation-dominated transitions. Therefore, it is clear that there is a sharp difference between perovskites $SrRuO_3$ and $BaRuO_3$ in terms of their critical behavior. The symmetry change from the orthorhombic to the cubic phase alone may not be sufficient to explain a T_c reduction from 160 to 60 K and the dramatic change of the critical behavior. To understand what is responsible for these fundamental changes between these two perovskite ruthenates, we have carried out measurements of magnetic and transport properties under pressure. Figure 2(a) shows a typical modified Arrott plot of the perovskite $BaRuO_3$ under pressure. Critical components as obtained from M_s vs T and χ_0^{-1} vs T in Fig. 2(b) are plotted as a function of pressure in Fig. 2(c). High pressure which reduces the Ru-O bond length within the cubic symmetry, does not change the critical behavior of the perovskite $BaRuO_3$ back to the mean-field universality class; instead, it enhances critical fluctuations at $T > T_c$ by increasing γ of Fig. 2(c) and leaves no clear sign how the β parameter changes within the accuracy provided in our experiment. The effect of nonhydrostatic stress on the critical behavior should be negligible since the highest pressure used is below the solidification pressure $P \approx 0.9$ GPa of 3M Florinert.

In the same way [9] as in $SrRuO_3$, $\rho(T)$ of $BaRuO_3$ shows an anomaly at T_c, see Fig. 3(a). As monitored by the anomaly of $d\rho/dT$ versus T in Fig. 3(b), T_c reduces under pressure at lower pressures, which is consistent with the result of the critical behavior analysis in Fig. 2(c). It is interesting that T_c of $BaRuO_3$ drops dramatically at low pressures; it saturates at $P > 3$ GPa and the magnitude of the anomaly of $d\rho/dT$ at T_c collapses as pressure increases. In contrast, a constant $dT_c/dP \approx -7$ K/GPa and no sign of T_c saturation has been obtained in the bulk sample $SrRuO_3$ [14,15]. These two features of $BaRuO_3$ are characteristic of a two-phase coexistence. We have confirmed the collapse of the ferromagnetism by a measurement of ac magnetic susceptibility under pressure in Fig. 3(c). The signal at T_c reduces dramatically with pressure, it falls to the background at 8 GPa. The small hump of χ at 12 K under 8 GPa is due to the magnetic contribution from the WC anvils since it is also shown in the measurements under lower pressures. This signal is enhanced under pressure since anvils move closer to the coils. The perovskite $BaRuO_3$ is terminated by the emergence of a two-phase region consisting of the ferromagnetic phase and a paramagnetic metallic phase under high pressure, which shows that the transition to a paramagnetic

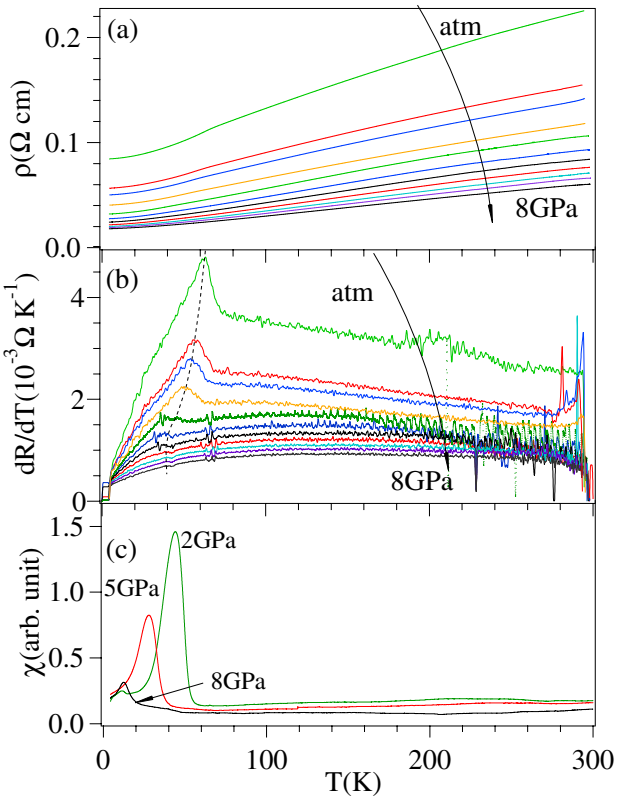

FIG. 3 (color online). (a) Temperature dependence of resistivity of $BaRuO_3$ under different pressures from ambient pressure to 8 GPa; (b) temperature dependence of the derivative dR/dT at pressures corresponding to that in (a); the dashed line is a guide to eye to track the peak position; (c) temperature dependence of ac magnetic susceptibility under three pressures; a primary-secondary method with $H = 704$ Hz and a lock-in amplifier SR 830 were used in this measurement.

metallic phase is first order. This important observation distinguishes clearly the ferromagnetic phase of the perovskite $BaRuO_3$ from the VWIEF $ZrZn_2$, for instance, which remains a single phase while T_c is suppressed under pressure [16,17]. Moreover, the pressure dependence of T_c of the cubic $BaRuO_3$ in Fig. 4 does not follow the prediction of $T_c(P) = T_c(0)(1 - P/P_c)^{0.5}$ from a model of VWIEF [18]. Although the difference between the ferromagnetic $BaRuO_3$ and the VWIEF $ZrZn_2$ is distinct, the two perovskites $BaRuO_3$ and $SrRuO_3$ share several common characteristics such as a similar structure, similar μ_{eff} in the paramagnetic phase, and a higher saturation moment at low temperature. T_c in the bulk sample $SrRuO_3$, however, does not saturate and no two-phase region has been observed at the highest pressure so far. $SrRuO_3$ appears to have a narrower bandwidth than that of $BaRuO_3$, so it stays away from the transition to a paramagnetic metallic phase. The question is whether this difference is enough to account for a dramatic change of critical behavior between them.

The ferromagnetic phase in the perovskite $BaRuO_3$ terminates under pressure at a temperature that is significantly higher than the lowest T_c of $ZrZn_2$ under pressure. $ZrZn_2$ exhibits quantum critical behavior in the vicinity where T_c vanishes under pressure [19]. One of characteristics for a phase with quantum critical fluctuations is to show the power law $\rho = \rho_0 + T^n$ ($n < 2$) at low temperatures where a charge or spin ordered phase is suppressed [20], which has been observed in many systems, for example, $CeCu_2Si_2$ [21], URu_2Si_2 [22], SmB_6 [23], MnSi [24], and $PrNiO_3$ [25]. A power-law analysis on the $\rho(T)$ of $BaRuO_3$ was made and fitting results are shown in Fig. 5. The exponent n as a function of pressure in Fig. 4 shows an interesting evolution from $n \approx 1.85$, which is close to $n = 2$ for the Fermi-liquid (FL) phase at ambient pressure, to $n \approx 1.4$ of a non-Fermi-liquid (NFL) phase at a pressure where the ferromagnetic phase collapses. In contrast, a Fermi-liquid phase has been reported for $SrRuO_3$ [26]. This observation indicates that quantum critical fluctuations dominate at low temperatures not only near the vicinity where the ferromagnetic phase collapses but also over a broad pressure range in $BaRuO_3$; the influence can also be seen even at ambient pressure. Although the effect of quantum critical fluctuations may become negligible at a

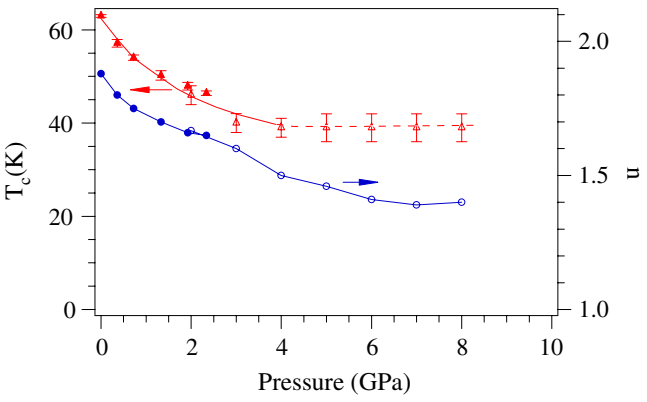

FIG. 4 (color online). Pressure dependences of T_c and exponent n in the $\Delta\rho = T^n$ of $BaRuO_3$. Points of T_c and n marked with solid symbols were obtained in a piston-cylinder setup; those with open symbols were obtained in the cubic anvil setup in which a stable seal is established at $P \geq 2$ GPa. The two-phase region is marked by a dashed line in the curve of T_c versus P.

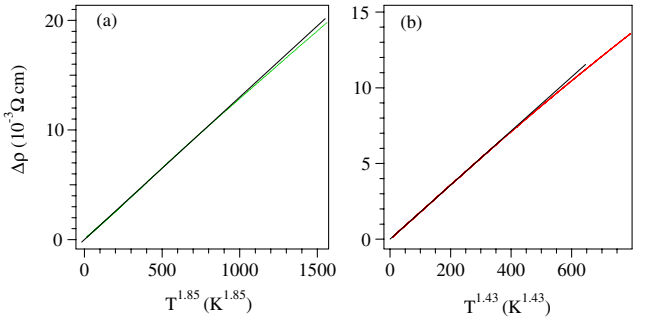

FIG. 5 (color online). The plot of $\Delta\rho = \rho - \rho_0$ versus T^n of $BaRuO_3$ under (a) ambient pressure and (b) 8 GPa.

temperature as high as T_c for this compound, thermodynamically driven phase fluctuations between the ferromagnetic phase and a paramagnetic phase, which is clearly seen at high pressures, could influence the critical behavior for the magnetic transition.

In comparison with the orthorhombic $SrRuO_3$, the bandwidth broadens significantly in the cubic $BaRuO_3$ due to a 180° Ru-O-Ru bond angle and the large difference of electronegativity between Sr^{2+} and Ba^{2+}, which may contribute to a reduced saturation magnetic moment $0.8\mu_B$/Ru from $1.4\mu_B$/Ru in $SrRuO_3$ and a dramatic reduction of T_c observed in the cubic $BaRuO_3$ in accordance with a general argument of itinerant-electron ferromagnetism [1]. However, these factors should make the magnetic transition of $BaRuO_3$ closer to the mean-field universality class than $SrRuO_3$ in the context of a model of VWIEF. We are forced to look for an alternative explanation for critical fluctuations observed in $BaRuO_3$. Critical fluctuations are confined within a temperature range determined by the Ginzburg criterion $t_G = (T_G - T_c)/T_c \sim \Delta C^{-2}\xi_0^{-6}$, where ΔC is the specific heat discontinuity at T_c and ξ_0 is the coherence length at zero temperature. The critical scattering at T_c causes an anomaly in $\rho(T)$ as seen more clearly in the curve of $d\rho/dT$ versus T in Fig. 3(b). The anomaly of $d\rho/dT$ versus T resembles the profile of C_p vs T at T_c as predicted by Fisher and Langer [27]. A similar behavior occurs in both perovskites $SrRuO_3$ and $BaRuO_3$. Therefore, we can have an estimation of the t_G change between them by comparing the $\Delta/(d\rho/dT)$ at T_c, where Δ is the discontinuity of $d\rho/dT$ at T_c: $\Delta/d\rho/dT \approx 0.7$ in $SrRuO_3$ [9] and ≈ 0.2 in $BaRuO_3$. This comparison indicates that critical fluctuations in $BaRuO_3$ should be present in a scaling temperature range that is about 1 order of magnitude higher than that of $SrRuO_3$. Also, t_G is expected to increase under pressure since the magnitude of the anomaly in $d\rho(T)/dT$ reduces dramatically as pressure increases, as can be seen in Fig. 3(b). This comparison and the pressure dependence are consistent with the significantly enhanced critical fluctuations observed in the perovskite $BaRuO_3$ at ambient pressure and under high pressure.

Although we cannot borrow the same mathematics used in the VWIEF system to justify the isothermal M^2 vs H/M observed in the perovskite $SrRuO_3$, a general argument [28] how the mean-field model breaks down offers an important guide to this problem. The larger the number of spins that interact with a test spin, the more the test spin sees an effective average or mean field. The fluctuations are large and important for a test spin with a reduced number of neighboring spins. Whereas $SrRuO_3$ and $BaRuO_3$ share a similar number of near-neighbor Ru atoms, the fraction of Ru atoms carrying a spin is apparently reduced as the transition to Pauli paramagnetism is approached in $BaRuO_3$. A fast probe such as neutron inelastic scattering or NMR [29] could be useful to verify this key difference between $SrRuO_3$ and $BaRuO_3$.

In conclusion, two perovskites $SrRuO_3$ and $BaRuO_3$ share some common characteristics in both their paramagnetic and ferromagnetic phases, but they are sharply different in terms of critical behavior at the ferromagnetic transition. The transition in $SrRuO_3$ falls into the mean-field universality class whereas $BaRuO_3$ exhibits significant critical fluctuations as described by the 3D Heisenberg model. Moreover, its critical fluctuations are enhanced under pressure. The ferromagnetic phase in $BaRuO_3$ collapses under high pressure in a first-order transition to a paramagnetic phase. A non-Fermi-liquid behavior due to quantum critical fluctuations has been found at low temperatures in $BaRuO_3$ under a broad range of pressure. Severe fluctuations in the fraction of Ru that carry a spin on transitioning with pressure to a paramagnetic phase in $BaRuO_3$ destroy the uniform ferromagnetic coupling, which enhances the critical fluctuations at the magnetic transition in $BaRuO_3$.

This work was supported by NSF in the U.S. and by KAKENHI (19GS0205, 19840017) in Japan.

*jszhou@mail.utexas.edu

[1] E. P. Wohlfarth, J. Appl. Phys. **39**, 1061 (1968).
[2] E. A. Yelland *et al.*, Phys. Rev. B **72**, 184436 (2005).
[3] M. Seeger *et al.*, Phys. Rev. B **51**, 12 585 (1995).
[4] F. Y. Yang *et al.*, Phys. Rev. B **63**, 092403 (2001).
[5] H. Yanagihara *et al.*, Phys. Rev. B **65**, 092411 (2002).
[6] D. Kim *et al.*, Phys. Rev. Lett. **89**, 227202 (2002).
[7] K. Ghosh *et al.*, Phys. Rev. Lett. **81**, 4740 (1998).
[8] W. Li *et al.*, Phys. Rev. B **75**, 012406 (2007).
[9] D. Kim *et al.*, Phys. Rev. B **67**, 100406 (2003).
[10] L. Klein *et al.*, Phys. Rev. Lett. **77**, 2774 (1996).
[11] G. Cao *et al.*, Phys. Rev. B **56**, 321 (1997).
[12] C.-Q. Jin *et al.*, Proc. Natl. Acad. Sci. U.S.A. **105**, 7115 (2008).
[13] N. Mori *et al.*, High Press. Res. **24**, 225 (2004).
[14] J. J. Hamlin *et al.*, Phys. Rev. B **76**, 014432 (2007).
[15] J. Pietosa, Phys. Rev. B **77**, 104410 (2008).
[16] M. Uhlarz *et al.*, Phys. Rev. Lett. **93**, 256404 (2004).
[17] F. M. Grosche *et al.*, Physica (Amsterdam) **206B & 207B**, 20 (1995).
[18] T. F. Smith *et al.*, Phys. Rev. Lett. **27**, 1732 (1971).
[19] S. Takashima *et al.*, J. Phys. Soc. Jpn. **76**, 043704 (2007).
[20] A. Rosch, Phys. Rev. Lett. **82**, 4280 (1999).
[21] H. Q. Yua *et al.*, Science **302**, 2104 (2003).
[22] K. H. Kim *et al.*, Phys. Rev. Lett. **91**, 256401 (2003).
[23] S. Gabani *et al.*, Phys. Rev. B **67**, 172406 (2003).
[24] C. Pfleiderer *et al.*, Nature (London) **414**, 427 (2001).
[25] J.-S. Zhou *et al.*, Phys. Rev. Lett. **94**, 226602 (2005).
[26] A. P. Mackenzie *et al.*, Phys. Rev. B **58**, R13318 (1998).
[27] M. E. Fisher and J. S. Langer, Phys. Rev. Lett. **20**, 665 (1968).
[28] P. Chaikin and T. C. Lubensky, *Principles of Condensed Matter Physics* (Cambridge University Press, New York, 1995), 1st ed.
[29] K. Yoshimura *et al.*, Phys. Rev. Lett. **83**, 4397 (1999).